Korean J. Chem. Eng., **31**(9), 1656-1660 (2014)
DOI: 10.1007/s11814-014-0097-0

pISSN: 0256-1115
eISSN: 1975-7220

Experimental determination and prediction of phase behavior for 1-butyl-3-methylimidazolium nonafluorobutyl sulfonate and carbon dioxide

Soon Kang Hong*, YoonKook Park*,†, and Dattaprasad Marutrao Pore**

*Department of Biological and Chemical Engineering, Hongik University, Sejong 339-701, Korea
**Department of Chemistry, Shivaji University, Kolhapur 416 004, India
(*Received 7 February 2014 • accepted 1 April 2014*)

Abstract−The vapor-liquid equilibrium of the binary system CO_2+1-butyl-3-methylimidazolium nonafluorobutyl sulfonate ([BMIM][NfO]) was measured over a temperature range of 298.2-323.2 K at intervals of 5.0 K for CO_2 mole fraction ranging from 0.137 to 0.900 using a high-pressure variable-volume view cell. The Peng-Robinson equation of state was then applied with two-parameter mixing rules over the same range and the results compared with the experimentally obtained data. Increasing the alkyl chain length in perfluorinated sulfonate from methyl to butyl markedly increased the CO_2 solubility. To investigate the effect of the number of fluorine atoms in the anion on the phase behavior of imidazolium based ionic liquid, these experimental results were then compared with those reported in previous experimental studies of 1-alkyl-3-methylimidazolium cations and with modeling data. It looks likely that both the number of fluorine atoms in the anion and the presence of S=O groups play an important role in designing CO_2-philic molecules.

Keywords: Carbon Dioxide, Phase Equilibrium, 1-Alkyl-3-methylimidazolium Nonafluorobutyl Sulfonate, VLE

INTRODUCTION

Based on their structural characteristics, several cation mother structures and a number of anion functional groups have been used to synthesize ionic liquids (ILs) in a variety of different forms, depending on the target application. The resulting high degree of flexibility for synthesizing different functional groups containing ionic liquids has meant that CO_2 capture in the presence of an appropriate IL has been widely studied [1-3]. However, without a better understanding of the fundamental thermodynamic properties of these systems it is not possible to extend the use of IL in CO_2 treatment, in particular to replace aqueous amine solutions, which suffer from serious drawbacks due to corrosion and high energy penalty for recovery.

Imidazolium is often utilized as a primary cation structure because it can serve as a mother structure to modify the cation by simply substituting 1 and/or 3 positions with a variety of functional groups [4]. There have been many studies on the influence of alkyl chain length in 1-alkyl-3-methylimidazolium [AMIM] cation containing IL on CO_2 solubility [5-8]. In particular, Shin and Lee [8] showed that the CO_2 solubility increases as the alkyl chain length increases from ethyl to octyl, maintaining the anion with trifluoromethyl sulfonate (TfO). This may be because a longer alkyl chain length increases the dispersion force, resulting in an enhanced interaction with CO_2 [9].

The influence of the anion on the CO_2 solubility seems to be far more important than that of its cation counterpart [7]. Since the affinity between CO_2 and fluorine is quite high at the molecular level [10], ILs containing fluorine as anions generally exhibit better results in terms of CO_2 solubility. Aki and coworkers [7] reported that at 298 K, the CO_2 solubility in 1-butyl-3-methylimidazolium (BMIM) cation based ILs increases in the following order: nitrate (NO_3)<dicyanamide (DCA)<tetrafluoroborate (BF_4) ~ phosphorous hexafluoride (PF_6)< (TfO)<bis(trifluoromethylsulfonyl)imide (Tf_2N)<(methide). However, to the best of our knowledge, as yet there have been no reports of the effect on CO_2 solubility of the perfluorinated alkyl chain length in the anion.

In this study, we measured the high-pressure phase equilibria of the 1-butyl-3-methylimidazolium nonafluorobutyl sulfonate ([BMIM][NfO]) and CO_2 binary system over a range of temperature and CO_2 mole fractions. To investigate the effect of the perfluorinated alkyl chain length in the anion, the phase equilibria of the [BMIM][NfO] and CO_2 binary system were compared to those of 1-butyl-3-mtheylimidazolium trifluoromethyl sulfonate ([BMIM][TfO]) and other fluorine atom containing ILs. The experimental phase equilibria data were then compared to those predicted by applying the Peng-Robinson equation of state (PR-EoS) and the van der Waals two-parameter mixing rule.

EXPERIMENTAL

1. Chemicals

1-Methylimidazole (≥99%), 1-bromobutane (99%), hexane (95%), toluene (99.8%), ethyl acetate and acetone were acquired from Sigma-Aldrich (St. Louis, MO, USA). Potassium nonafluorobutyl sulfonate (98%) was purchased from Wuhan Bright Chemical Co. (Hubei, China). The SFC grade carbon dioxide (99.999%) was purchased from Sebotech Inc. (Daejeon, Korea). All chemicals were used as received.

2. Synthesis

The synthesis of 1-butyl-3-methylimidazolium bromide, i.e., [BMIM][Br], and [BMIM][NfO], were carried out using a method similar to the one that we reported earlier [11]. Accordingly, 1-bromo

†To whom correspondence should be addressed.
E-mail: parky@hongik.ac.kr

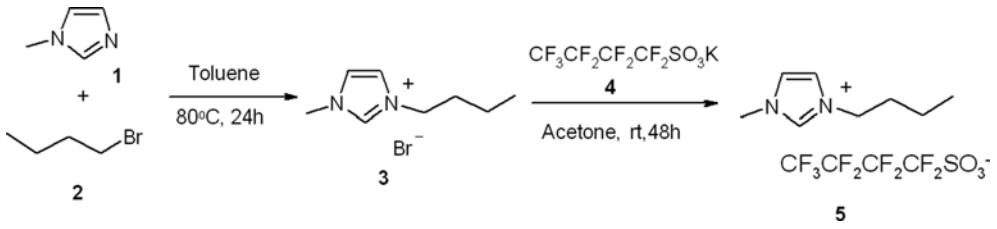

Scheme 1.

butane (55 mmol) was slowly added at 0 °C to a vigorously stirred solution of 1-methylimidazole (50 mmol) in toluene (25 cm^3). The quaternization reaction was carried out at 80 °C for 24 hours, and it was subsequently placed in a freezer at 0 °C for 4 hours. The toluene was decanted, and the remaining viscous oil was repeatedly washed with ethyl acetate, yielding a yellow oil. This oil was then dried in vacuum, and [BMIM][Br] was obtained in approximately 90% yield.

[BMIM][Br] (20 mmol) IL was dissolved in acetone and potassium nonafluorobutyl sulfonate (22 mmol) was added; the resulting mixture was stirred for 48 hours at room temperature. The thus-obtained suspension was filtered to remove the precipitated bromide salt and the solvent was evaporated under reduced pressure. Then it was dissolved in dichloromethane/chloroform and washed repeatedly with small volumes of water (30 cm^3) until the addition of $AgNO_3$ solution did not cause further precipitation of AgBr in the aqueous phase. The organic phase was then washed twice with water to ensure complete removal of the bromide salt. The solvent was removed in vacuum until no visible signs of the organic solvents or water remained, resulting in a 92% yield of the corresponding IL. The water content of [BMIM][NfO] product was measured by Karl Fischer moisture analysis and was found to be less than 300 ppm. Scheme 1 shows this synthesis.

Spectral data for IL: ^{1}H NMR ($CDCl_3$, 400 MHz): δ 0.92 (t, 3H), 1.33 (m, 2H), 1.84 (m, 2H), 3.95 (s, 3H), 4.17 (t, 2H), 7.33 (t, 1H, *J*=3.6 Hz), 7.37 (t, 1H, *J*=3.6 Hz), 9.08 (s, 1H); ^{13}C NMR ($CDCl_3$, 100 MHz): 13.36, 19.52, 32.12, 36.50, 50.04, 122.32, 123.84, 136.97; ^{19}F NMR ($CDCl_3$, 376 MHz): −80.99 (CF_3), −114.95 (CF_2), −121.73 (CF_2), −126.09 (CF_2).

3. Experimental Apparatus and Method

Vapor liquid equilibria (VLE) experiments were performed by using a high-pressure variable-volume view cell (described in detail elsewhere) [6,9]. The temperature and pressure were measured by a calibrated thermocouple with 0.1 K accuracy and a calibrated pressure indicator (Heise, model 901A, 0.07% accuracy), respectively. The procedure used was as follows. The contents in the view cell were stirred with a Teflon-coated magnetic bar during the whole experiment. A small amount (typically around 12 g) of the IL was loaded into the view cell. The air, along with dissolved gas and water, was removed from the IL by evacuating the cell at vacuum for at least three hours at room temperature. Once the upper portion of the view cell became entirely clear, a measured amount of CO_2 was introduced under constant temperature and pressure by using a syringe pump. The mass of the CO_2 admitted was calculated based on the difference in the volume and density [12] of the gas in the syringe pump before and after the CO_2 was introduced into the cell. The bubble point pressure was taken to be the pressure at which the first bubbles were observed. All measurements were made at least four times for each condition.

MODELING

ILs have a negligible vapor pressure, so it is reasonable to assume that there will be no IL present in the vapor phase. In an equilibrium, the fugacity of CO_2 in vapor phase and that in the IL-rich phase will be the same for constant temperature and pressure:

$$f_1^v = \hat{f}_1^{IL} \tag{1}$$

where f_1^v is the fugacity of CO_2 (1) in vapor phase and $\hat{f}_1^{IL}$ is the fugacity of the IL (2). Constructing an equation of state greatly facilitates the correlation of experimental data for binary mixtures, and the Peng-Robinson equation of state (PR-EoS) is widely used for practical applications. It can be expressed as:

$$P = \frac{RT}{v - b_m} - \frac{a_m}{v(v+b_m) + b_m(v-b_m)} \tag{2}$$

where a_m and b_m are the attractive and co-volume parameters, respectively, of the mixture. The pure component parameters a_i and b_i can be expressed as

$$a_i = \frac{0.45724 R^2 T_C^2}{P_C}[1 + \beta(1 - \sqrt{T_r})]^2 \tag{3}$$

$$\beta = 0.37464 + 1.54226\omega - 0.26992\omega^2 \tag{4}$$

$$b_i = \frac{0.0778 R T_C}{P_C} \tag{5}$$

The mixture parameters, a_m and b_m are computed using the mixing rules given by Eqs. (6) and (7):

$$a_m = \sum_{i=1}\sum_{j=1} x_i x_j a_{ij} \tag{6}$$

$$b_m = \sum_{i=1}\sum_{j=1} x_i x_j b_{ij} \tag{7}$$

where

$$a_{ij} = \sqrt{a_i a_j}(1 - k_{ij}) \tag{8}$$

$$b_{ij} = \frac{b_i + b_j}{2}(1 - l_{ij}) \tag{9}$$

The parameters $a_{ii}=a_i$ and $b_{ii}=b_i$ for a pure species are determined by Eqs. (3) and (5), respectively, and k_{ij} and l_{ij} are the binary interaction parameters.

While the critical properties of CO_2 are readily available in the literature [12], those of [BMIM][NfO] were calculated using the same method as that used by Valderrama and Robles [13] (Table 1). The experimentally obtained bubble point pressure data for the CO_2+

Table 1. Physical properties of chemicals

	Formula	Mw [g/mol]	T_C/K	P_C/MPa	ω	Ref.
[BMIM][NfO]	$C_{12}H_{15}N_2O_3F_9S$	438.3	1028.8	1.73	0.5151	This study[a]
[BMIM][BF_4]	$C_8H_{15}BF_4N_2$	226.0	632.3	2.04	0.8489	[13]
[BMIM][PF_6]	$C_8H_{15}F_2N_2P$	284.2	708.9	1.73	0.7553	[13]
[BMIM][TfO]	$C_8H_{15}N_2CF_3O_3S$	288.3	1016.3	2.94	0.3677	[13]
[BMIM][Tf_2N]	$C_{10}H_{15}N_3O_4F_9S_2$	419.4	1265.0	2.76	0.2656	[13]
[BMIM][methide]	$C_{12}H_{15}N_2O_6F_9S_3$	550.4	1571.4	2.40	0.1320	[21]
CO_2	CO_2	44.01	304.2	7.38	0.239	[12]

[a]The critical properties of ionic liquids are estimated by using a method from the literature [13]

[BMIM][NfO] binary system were correlated with the results predicted by the PR-EoS at each temperature. The software package PE 2000 [14] was used to approximate the VLE. To facilitate optimization, the objective function (OF) can be defined in terms of the average absolute relative deviation (AARD) for the liquid mole fraction, expressed as a percentage:

$$\mathrm{OF}=\frac{1}{\mathrm{N}}\sum_{i=1}^{N}\frac{\left|x_i^{exp}-x_i^{cal}\right|}{x_i^{exp}}\cdot 100 \tag{10}$$

where x_i^{cal} is the calculated mole fraction in the liquid phase and x_i^{exp} is the experimentally measured mole fraction in the liquid phase for a given temperature; N is the number of data points.

RESULTS AND DISCUSSION

1. Phase Equilibria of CO_2+[BMIM][NfO]

The bubble point pressures for [BMIM][NfO]+CO_2 were measured over the temperature range 298.2-323.2 K at intervals of 5 K. The experimental results are shown in Table 2. The error in the composition was obtained by the method reported by Ren and Scurto [15], and that in pressure was the standard deviation of the average for four independent experiments. Fig. 1 shows the bubble point pressure versus CO_2 mole fraction, along with the results of the PR-EoS for comparison. In general, the model and the experimental data are in good agreement. As the temperature increases, the pressure must also increase in order to dissolve a given amount of CO_2 in [BMIM][NfO], as Fig. 2 clearly shows.

At constant temperature, the solubility of CO_2 in [BMIM][NfO] increases with pressure, for example increasing from 0.205 at 2.35 MPa to 0.602 at 5.68 MPa at 308.2 K. This increase was expected based on previous results in the literature [16]. The correlation between the experimental VLE data and the PR-EoS with quadratic mixing rules was established and the binary interaction parameters determined at three different temperatures, are shown in Table 3.

2. Effect of CO_2 Solubility of the Alkyl Chain Length in the Perfluorinated Anion

The solubility of CO_2 in [AMIM][TfO] was determined by Shin and Lee [8] as the alkyl chain length in the imidazolium cation was systematically increased from ethyl to octyl. For the perfluorinated anion, our results showed that as the alkyl chain length increased, the solubility of CO_2 increased correspondingly. Compared to the pressure required to dissolve a 0.5367 mole fraction of CO_2 in [BMIM][TfO] at 303.85 K, 4.90 MPa [8], the pressure needed to dissolve a 0.5310 CO_2 mole fraction in [BMIM][NfO] at 303.2 K was lower at 4.45 MPa.

Fig. 3 shows the effect of the anion on the solubility of CO_2 with

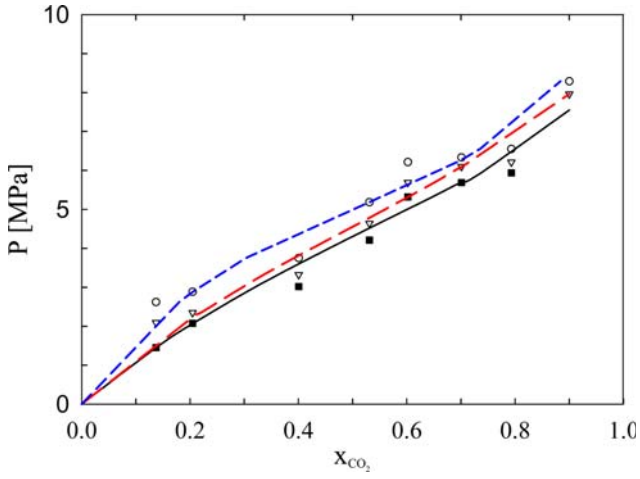

Fig. 1. P-x_1 diagram of CO_2 (1)+[BMIM][NfO] (2) system at different temperatures (■: 298.2 K; ▽: 308.2 K; ○: 318.2 K; the dotted blue line, dashed red line, and solid black line represent the modeling results for VLE at 318.2 K, 308.2 K, and 298.2 K, respectively).

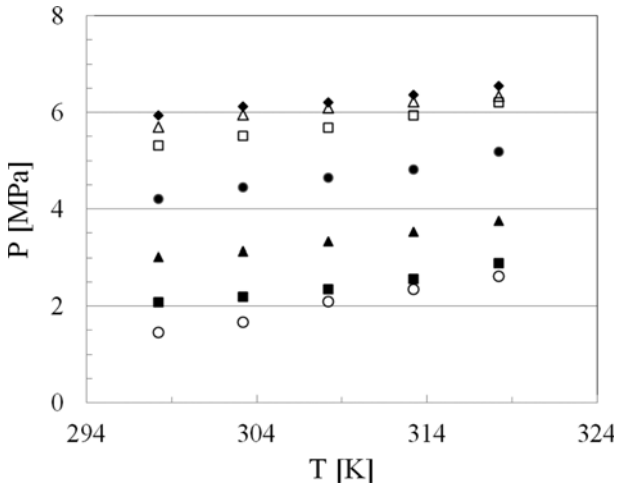

Fig. 2. Experimentally determined isopleths for different concentrations of the CO_2 (1)+[BMIM][NfO] (2) system. Legend ○: 0.1373; ■: 0.2048; ▲: 0.4007; ●: 0.5310; □: 0.6020; △: 0.7009; ◆: 0.7931.

Table 2. Experimentally determined bubble point pressures for CO_2 (1)+[BMIM][NfO] (2)

T/K	x_{CO2}	P [MPa]
298.2	0.1373±0.010	1.451±0.015
	0.2048±0.008	2.075±0.043
	0.4007±0.006	3.020±0.030
	0.5310±0.004	4.209±0.043
	0.6020±0.004	5.318±0.015
	0.7009±0.003	5.690±0.086
	0.7931±0.002	5.938±0.014
303.2	0.1373±0.010	1.662±0.020
	0.2048±0.008	2.193±0.018
	0.4007±0.006	3.123±0.032
	0.5310±0.004	4.449±0.041
	0.6020±0.004	5.518±0.015
	0.7009±0.003	5.954±0.036
	0.7931±0.002	6.123±0.015
	0.9000±0.001	7.800±0.018
308.2	0.1373±0.010	2.093±0.054
	0.2048±0.008	2.351±0.012
	0.4007±0.006	3.323±0.021
	0.5310±0.004	4.642±0.069
	0.6020±0.004	5.688±0.022
	0.7009±0.003	6.097±0.047
	0.7931±0.002	6.212±0.011
	0.9000±0.001	7.962±0.012
313.2	0.1373±0.010	2.348±0.015
	0.2048±0.008	2.565±0.025
	0.4007±0.006	3.523±0.014
	0.5310±0.004	4.818±0.030
	0.6020±0.004	5.931±0.007
	0.7009±0.003	6.226±0.051
	0.7931±0.002	6.357±0.015
	0.9000±0.001	8.115±0.030
318.2	0.1373±0.010	2.620±0.039
	0.2048±0.008	2.884±0.038
	0.4007±0.006	3.751±0.025
	0.5310±0.004	5.183±0.015
	0.6020±0.004	6.214±0.009
	0.7009±0.003	6.333±0.033
	0.7931±0.002	6.550±0.022
	0.9000±0.001	8.287±0.063
323.2	0.1373±0.010	2.851±0.015
	0.2048±0.008	3.045±0.014

[BMIM] as the counterpart cation at 313 K. Among the six fluorine containing anions in ILs that have now been characterized, [BMIM][NfO] exhibits the highest CO_2 solubility. Given that [BMIM][methide] and [BMIM][NfO] both yield better CO_2 solubilities than any of the other fluorine containing anions in ILs, it seems likely that the number of fluorine atoms in the anion plays a critical role in CO_2 solubility, with anions containing more fluorine atoms in their molecular structure having higher CO_2 solubilities. However, the number of fluorines alone is not sufficient to explain why [BMIM][PF_6] has

Table 3. The binary interaction parameters for CO_2+[BMIM][NfO] system

T/K	Number of data points	Interaction parameters	
		k_{12}	l_{12}
298.2	7	0.04387	−0.02660
308.2	8	0.02018	−0.02966
318.2	8	−0.01890	−0.04747

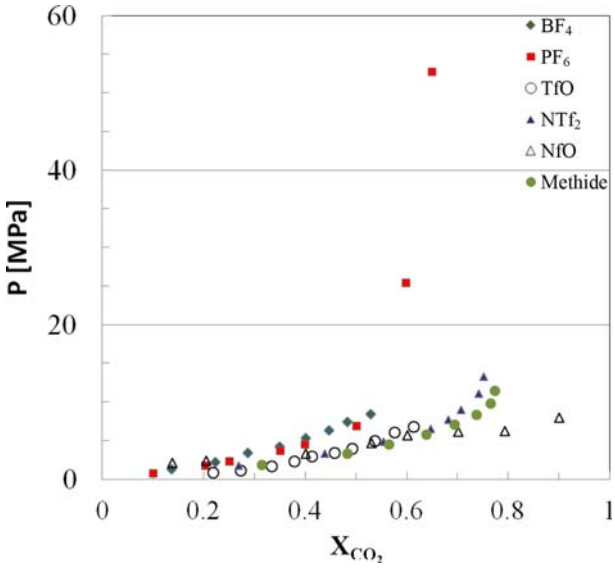

Fig. 3. Solubility of CO_2 in various anions for a [BMIM] cation containing IL at 313 K ([BF_4]: ref. 7; [PF_6]: ref. 18; [TfO]: ref. 8; [Tf_2N]: ref. 7; [NfO]: this study; [methide]: ref. 7).

a lower CO_2 solubility than other ILs such as [BMIM][Tf_2N], given that it has no fewer than six fluorine atoms in its anion structure. As Wang et al. [17] suggested, this may not depend solely on the number of fluorine atoms in the IL structure and the presence of S=O groups may play a synergistic role.

A similar trend has been reported by a number of different research groups. In the case of 1-hexyl-3-methylimidazolium (HMIM) cation-based ILs, the CO_2 solubility at 298.2 K also depends on the anion, increasing in the following order [17-20]: tris(heptafluoropropyl)trifluorophosphate [pFAP]>tris(pentafluoroethyl)trifluorophosphate [eFAP]>[Tf_2N]>[PF_6]. As in the case of [BMIM] based ILs, [HMIM] based ILs exhibit their highest CO_2 solubility when as many as 24 fluorine atoms are attached in the anion, [pFAP]. Interestingly, the number of fluorine atoms in the anion molecular structure, as well as the presence of S=O groups, appears to be remarkably important when designing CO_2-philic ILs. The alkyl chain length on the cation, the number of fluorine atoms on the anion, and the presence of S=O groups all appear to serve important roles in ILs targeting CO_2 capture.

CONCLUSIONS

We examined the high-pressure phase behavior of the binary system CO_2+[BMIM][NfO] using a high-pressure variable-volume view cell. Results of modeling utilizing the Peng-Robinson equation of

state in conjunction with two-parameter mixing rules showed good correlation with the experimental data. At constant temperature, the solubility of CO_2 in [BMIM][NfO] increased with pressure, as expected based on previous reports in the literature. The CO_2 solubility depends on the number of fluorine atoms in the anion, but the presence of S=O also plays a critical role in enhancing solubility. In general, longer alkyl chain length in the cation, higher numbers of fluorine atoms in the anion, and the presence of S=O groups all appear to be important factors in the design of more effective ILs for capturing CO_2.

ACKNOWLEDGEMENT

This research was supported by Basic Science Research Program through the National Research Foundation of Korea (NRF) funded by the Ministry of Education, Science and Technology (2011-0007725).

REFERENCES

1. E. Privalova, M. Nurmi, M. S. Marañón, E. V. Murzina, P. Mäki-Arvela, K. Eränen, D. Y. Murzin and J. P. Mikkola, *Sep. Purif. Technol.*, **97**, 42 (2012).
2. D. Kodama, M. Kanakubo, M. Kokubo, T. Ono, H. Kawanami, T. Yokoyama, H. Nanjo and M. Kato, *J. Supercrit. Fluids*, **52**, 189 (2010).
3. D. Wappel, G. Gronald, R. Kalb and J. Draxler, *Int'l. J. Greenhouse Gas Control*, **4**, 486 (2010).
4. D. W. Seo, Y. D. Lim, S. H. Lee, S. C. Ur and W. G. Kim, *Bull. Korean Chem. Soc.*, **32**, 2633 (2011).
5. M. S. Shannon and J. E. Bara, *Ind. Chem. Eng. Res.*, **50**, 8665 (2011).
6. S. Hwang, Y. Park and K. Park, *J. Chem. Thermodyn.*, **43**, 339 (2011).
7. S. N. V. K. Aki, B. R. Mellein, E. M. Sauer and J. F. Brennecke, *J. Phys. Chem. B*., **108**, 20355 (2004).
8. E.-K. Shin and B. C. Lee, *J. Chem. Eng. Data*, **53**, 2728 (2080).
9. S. Hwang, Y. Park and K. Park, *J. Chem. Eng. Data*, **57**, 2160 (2012).
10. P. Bell, A. J. Thote, Y. Park, R. B. Gupta and C. B. Roberts, *Ind. Eng. Chem. Res.*, **42**, 6280 (2003).
11. D. S. Gaikwad, Y. Park and D. M. Pore, *Tetrahedron Lett.*, **53**, 3077 (2012).
12. http://webbook.nist.gov/chemistry/fluid accessed on 28 December 2012.
13. J. O. Valderrama and P. A. Robles, *Ind. Eng. Chem. Res.*, **46**, 1338 (2007).
14. O. Pfohl, S. Petkov and G. Brunner, *PE 2000-A powerful tool to correlate phase equilibria*, Herbert Utx Verlag, Muchen (2000).
15. W. Ren and A. M. Scurto, *Rev. Sci. Instrum.*, **78**, 125104 (2007).
16. M. Yazdizadeh, F. Rahmani and A. A. Forghani, *Korean J. Chem. Eng.*, **28**, 246 (2011).
17. X. Wang, J. Chen and J. Mi, *Ind. Eng. Chem. Res.*, **52**, 954 (2013).
18. A. Shariati, K. Gutkowski and C. J. Peters, *AIChE J.*, **51**, 1532 (2005).
19. Y. S. Kim, W. Y. Choi, J. H. Jang, K. P. Yoo and C. S. Lee, *Fluid Phase Equilib.*, **228-229**, 439 (2005).
20. M. J. Muldoon, S. Aki, J. L. Anderson, J. K. Dixon and J. F. Brennecke, *J. Phys. Chem. B.*, **111**, 9001 (2007).
21. J. O. Valderrama, W. W. Sanga and J. A. Lazzus, *Ind. Eng. Chem. Res.*, **47**, 1318 (2008).